



Triphenylamine-based organic dyes containing a 1,2,3-triazole bridge for dye-sensitized solar cells via a 'Click' reaction

Tainan Duan, Ke Fan, Yang Fu, Cheng Zhong, Xingguo Chen*, Tianyou Peng*, Jingui Qin

Hubei Key Laboratory on Organic and Polymeric Opto-electronic Materials, and Department of Chemistry, Wuhan University, Wuhan 430072, China

ARTICLE INFO

Article history:

Received 21 September 2011

Received in revised form

18 November 2011

Accepted 19 November 2011

Available online 7 December 2011

Keywords:

Dye-sensitized solar cells (DSSCs)

'Click' reaction

Organic dye

1,2,3-Triazole

Triphenylamine

Photovoltaic properties

ABSTRACT

Three new organic dyes with one, two and three branched D- π -A structures derived from an electron donating triphenylamine core and connected by 1,2,3-triazole group to an electron deficient cyanoacrylate system have been conveniently synthesized via a 'Click' reaction. It was found that all three dyes show UV-vis absorptions in the 300–500 nm range with high molar extinction coefficients. A red-shift of UV-vis absorption band was observed in the solid thin film compared with the dioxane solution. Dye-sensitized solar cell devices based on the dyes were fabricated and tested. The one branched triphenylamine-based dye exhibits the highest energy conversion efficiency. Increase of the branched D- π -A structure around the triphenylamine core results in the decrease of energy conversion efficiency of the dyes, which can be attributed to less attachment of the dyes onto TiO₂ photoanode with the enlarged molecular size of the corresponding multibranch structure.

© 2011 Elsevier Ltd. All rights reserved.

1. Introduction

In nowadays the fast growing world-wide demand for energy and rapidly depleting fossil fuel energy sources has greatly encouraged scientists to explore and develop renewable and environmentally friendly energy sources, especially low cost direct use photoelectric conversion devices. Compared with the traditional silicon-based photovoltaic devices, dye-sensitized solar cells (DSSCs) exhibit many advantages such as easily structural modification and relatively low production costs, etc. Thus DSSCs have attracted great attention since their first report by O'Regan and Grätzel in 1991 [1] and have become one of the major competitors among the high performance future photovoltaic devices [2].

As one of the most crucial factors that influence the performance of DSSC, the sensitizing dyes involve various types of molecules from synthetic metal complexes [3] to natural dyes [4]. Also, tremendous new synthetic metal-free organic dyes [5,6] have been developed and employed as the sensitizer in DSSCs. Among them Ru(II)-based complex dyes remain dominant in photoelectronic conversion efficiency [7]. However, the inconvenient purification and high cost of Ru-based dyes limit their development compared to the metal-free organic dyes. Even though none of the

pure organic dyes has surpassed the conversion efficiency of the Ru-based sensitizers at present [8], they still have attracted considerable attention. Enormous studies have been devoted to design novel structural dyes, to clarify the relationship between the structure and properties and to optimize the DSSC devices [6,9].

In the synthesis of new DSSC dyes, the triphenylamine (TPA)-based structure has been widely employed to build metal-free organic dyes and it has been successfully proved to show high conversion efficiency in DSSC devices [10–14] since it can both enhance the hole-transporting ability of the materials and inhibit the aggregation of the dyes with its non-planar structure. Generally, the crucial step for synthesizing this kind of dye is to link the donor group (triphenylamine) and spacer group. This process is commonly performed via Palladium-catalyzed coupling reaction with some aromatic boric acids (borates) [12] or stannanes [14], which are both costly and require delicate handling. Recently, the Cu(I) catalyzed alkyne-azide 'Click' reaction introduced by Sharpless and co-workers [15] has been widely used in the design and synthesis of optoelectronic materials and affords a good way to achieve target molecules under mild reaction conditions with high efficiency [16–18]. In this paper three new triphenylamine-based organic dyes (**DH-1**, **DH-2** and **DH-3** shown in Fig. 1) have been synthesized, and the 1,2,3-triazole group as a bridge has been introduced into the π -conjugate skeleton for these DSSCs sensitizers via a 'Click' reaction. The

* Corresponding authors. Tel.: +86 27 68755655.

E-mail addresses: xgchen@whu.edu.cn (X. Chen), typeng@whu.edu.cn (T. Peng).

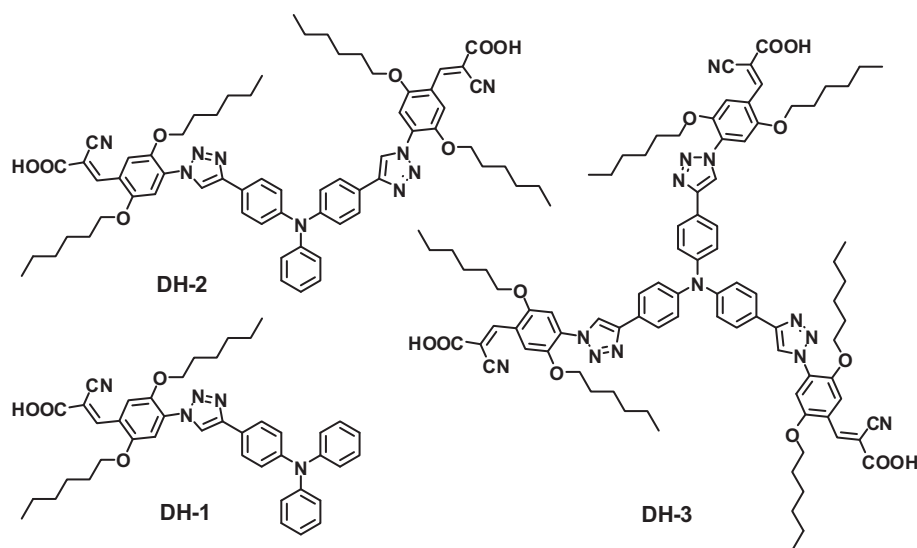


Fig. 1. Molecular structures of **DH-1**, **DH-2** and **DH-3** dyes.

photophysical properties, electrochemical properties and photo-voltaic properties have been investigated.

2. Experimental section

2.1. Equipments and materials

^1H NMR and ^{13}C NMR spectra were measured with a Varian MERCURY-VX300 in CDCl_3 or in $\text{DMSO}-d_6$ with TMS as internal reference. UV–vis absorption spectroscopy was performed on a Shimadzu UV-3600 spectrophotometer. The electrochemical behavior of the **DH** dyes was investigated using cyclic voltammetry (CV) on a CHI600A electrochemical work station. The elemental analysis was carried out on a CARLOERBA-1106 microelemental analyzer. Mass spectra were recorded with a VJ-ZAB-3F-Mass spectrometer or a Bruker 320-MS triple quadrupole mass spectrometer.

The catalyst of $\text{Pd}(\text{PPh}_3)_4$ was synthesized in our own lab, and anhydrous THF used in Schlenk system was dried and purified by reflux with Na–K alloy. Some other reagents and solvents were commercially purchased without further purification before use. Compounds **1** [19], **2** [19], **3** [20], **6** [21], **7** [21] and **8** [21] were prepared according to the corresponding literatures.

2.2. Synthesis of the intermediates and **DH** dyes

4-Azido-2,5-bis(hexyloxy)benzaldehyde (4): To solution of 2-(4-bromo-2,5-bis(hexyloxy)phenyl)-1,3-dioxane (**2**, 8.10 g, 18.2 mmol) in 80 mL of anhydrous THF, 8.00 mL of *n*-BuLi (2.5 M solution in hexane, 20.0 mmol) was added dropwise at -78°C . After stirring for 40 min 4-methylbenzenesulfonyl azide (**3**, 3.95 g, 20.0 mmol) in 10 mL of anhydrous THF was added dropwise to the mixture and kept stirring for 4 h at -78°C . Later, the reaction system was gradually warmed to -10°C and then excessive aqueous solution of sodium pyrophosphate was poured into the vessel. And then the cooling bath was removed and the mixture was stirred continuously for 12 h at room temperature. The resulting mixture was extracted with ether (40 mL \times 2), the organic phase was washed with brine, and then mixed with 2 M HCl (60 mL) to stir for 6 h. Finally, the crimson organic phase was dried over anhydrous Na_2SO_4 and the solvent was evaporated. The final product (**4**, yellow oil) was obtained by chromatography. Yield, 5.52 g (87%). ^1H

NMR (300 MHz, CDCl_3): δ 10.35 (s, 1H), 7.31 (s, 1H), 6.51 (s, 1H), 4.01 (t, 2H), 3.98 (t, 2H), 1.81–1.72 (m, 4H), 1.46–1.34 (m, 12H), 0.91–0.90 (m, 6H). ^{13}C NMR (75 MHz, CDCl_3): δ 188.5, 157.0, 146.6, 136.2, 121.6, 110.8, 105.6, 69.9, 69.4, 31.7, 29.2, 29.1, 25.9, 22.8, 14.2. MS (ESI): $m/z = 347.2$.

3-(4-Azido-2,5-bis(hexyloxy)phenyl)-2-cyanoacrylic acid (5): Compound **4** (3.47 g, 10.0 mmol), cyanoacetic acid (2.55 g, 30.0 mmol) and piperidine (several drops) were added to 30 mL of MeCN and the mixture was heated under reflux for 12 h. Then the solution was acidified with 2 M HCl (20 mL) and extracted with CH_2Cl_2 . The organic phase was dried over anhydrous Na_2SO_4 . The solvent was removed and the residue was purified on a silica gel column with chloroform as eluent to obtain the crude product. The pure product (**5**) (crimson solid) was obtained through recrystallization. Yield, 3.68 g (89%). ^1H NMR (300 MHz, CDCl_3): δ 8.78 (s, 1H), 8.01 (s, 1H), 6.48 (s, 1H), 4.08 (d, 2H), 3.97 (d, 2H), 1.85–1.80 (m, 4H), 1.47–1.35 (12H), 0.92–0.91 (6H). ^{13}C NMR (75 MHz, CDCl_3): δ 168.6, 155.2, 149.5, 146.5, 136.5, 116.9, 116.5, 111.9, 98.5, 70.0, 69.8, 31.8, 31.7, 29.1, 26.0, 25.8, 22.8, 14.2. MS (ESI): $m/z = 413.9$. $\text{C}_{22}\text{H}_{30}\text{N}_4\text{O}_4$ ($M_w = 414.50$): calcd. C, 63.75; H, 7.30; N, 13.52; found C, 63.40; H, 7.01; N, 13.14.

2-Cyano-3-(4-(4-(4-(diphenylamino)phenyl)-1H-1,2,3-triazol-1-yl)-2,5-bis(hexyloxy)phenyl)acrylic acid (DH-1): N,N-diphenyl-4-Ethynylaniline (**6**, 0.269 g, 1 mmol), compound **5** (0.414 g, 1 mmol), NaHCO_3 (4.20 mg, 0.05 mmol) and ascorbic acid (8.81 mg, 0.05 mmol) were dissolved in the mixed solvent of THF– H_2O (20 mL, $V_{\text{THF}}/V_{\text{H}_2\text{O}} = 2:1$), and an aqueous solution of $\text{CuSO}_4 \cdot 5\text{H}_2\text{O}$ (12.5 mg, 0.05 mmol in 1 mL water) was added to it under Ar atmosphere. After stirring for 8 h, the mixture was extracted with ether (30 mL \times 3) and organic phase was dried over anhydrous Na_2SO_4 . The solvent was removed and the residue was purified on a silica gel column with ethyl acetate as eluent to obtain the crude product. Pure **DH-1** dye (orange powder) was obtained through recrystallization from CH_2Cl_2 /ethyl acetate. Yield, 0.581 g (85%). ^1H NMR (300 MHz, $\text{DMSO}-d_6$): δ 8.87 (s, 1H), 8.32 (s, 1H), 7.93 (s, 1H), 7.82 (d, 2H), 7.50 (s, 1H), 7.33 (t, 4H), 7.10–7.04 (m, 8H), 4.10 (t, 2H), 4.05 (t, 2H), 1.75–1.69 (m, 8H), 1.42–1.19 (m, 8H), 0.86–0.75 (m, 6H). ^{13}C NMR (75 MHz, CDCl_3): δ 164.9, 151.4, 146.9, 146.7, 146.0, 142.8, 142.2, 128.9, 127.9, 126.93, 125.9, 123.8, 122.9, 122.7, 122.1, 121.3, 118.2, 113.1, 111.8, 108.0, 69.0, 68.7, 30.7, 28.3, 25.0, 24.8, 21.8, 13.6, 13.5. MS (ESI): $m/z = 683.6$. $\text{C}_{42}\text{H}_{45}\text{N}_5\text{O}_4$ ($M_w = 683.84$): calcd. C, 73.77; H, 6.63; N, 10.24. found C, 73.83; H, 7.04; N, 10.67.

3,3'-(4,4'-(4,4'-(4,4'-(Phenylazanediy)bis(4,1-phenylene))-bis(1H-1,2,3-triazole-4,1-diyl))bis(2,5-bis(hexyloxy)-4,1-phenylene))bis(2-cyanoacrylic acid) (**DH-2**): The synthetic procedure of **DH-2** was similar to **DH-1**, in which N,N-bis(4-ethynylphenyl)-phenylamine (**7**, 0.146 g, 0.5 mmol) was instead of **6** and compound **5** (0.414 g, 1 mmol) was used 2 times that of **7**. Pure **DH-2** dye (brown solid) was directly obtained by recrystallization after acidification without column chromatography. Yield, 0.431 g (77%). $^1\text{H NMR}$ (300 MHz, $\text{DMSO-}d_6$): δ 8.71 (s, 2H), 8.54 (s, 2H), 7.99 (s, 2H), 7.77 (d, 4H), 7.54 (s, 2H), 7.32 (t, 2H), 7.11–7.08 (m, 7H), 4.07 (t, 4H), 4.05 (t, 4H), 1.78–1.74 (m, 16H), 1.45–1.23 (m, 16H), 0.89–0.78 (m, 12H). $^{13}\text{C NMR}$ (75 MHz, $\text{DMSO-}d_6$): δ 161.5, 150.9, 145.1, 145.1, 144.6, 141.1, 140.9, 127.9, 127.6, 124.5, 122.8, 122.6, 121.7, 119.4, 118.4, 114.5, 111.1, 106.1, 102.0, 67.5, 67.4, 30.7, 28.3, 25.0, 24.8, 21.8, 13.6, 13.4. MS (ESI): $m/z = 1121.8$. $\text{C}_{66}\text{H}_{75}\text{N}_9\text{O}_8$ ($M_w = 1122.36$): calcd. C, 70.63; H, 6.74; N, 11.23; found C, 70.43; H, 7.18; N, 11.27.

3,3',3''-(4,4',4''-(4,4',4''-(4,4',4''-Nitrilotris(benzene-4,1-diyl))-tris(1H-1,2,3-triazole-4,1-diyl))tris(2,5-bis(hexyloxy)benzene-4,1-diyl))tris(2-cyanoacrylic acid) (**DH-3**): The synthetic procedure of **DH-3** was similar to **DH-1** and **DH-2**, in which tris(4-ethynylphenyl)amine (**8**, 0.158 g, 0.5 mmol) was instead of **6** or **7** and compound **5** (0.621 g, 1.5 mmol) was used 3 times that of **8**. Pure **DH-3** dye (dark red–brown solid) was obtained by recrystallization after acidification without column chromatography. Yield, 0.677 g (87%). $^1\text{H NMR}$ (300 MHz, $\text{DMSO-}d_6$): δ 8.65 (s, 3H), 8.56 (s, 3H), 7.92 (s, 3H), 7.82 (d, 6H), 7.53 (s, 3H), 7.29 (d, 6H), 4.09 (t, 6H), 4.07 (t, 6H), 1.81–1.76 (m, 24H), 1.49–1.24 (m, 24H), 0.92–0.82 (m, 18H). $^{13}\text{C NMR}$ (75 MHz, CDCl_3): δ 160.9, 157.9, 154.8, 151.4, 149.1, 146.1, 143.6, 142.9, 134.0, 136.1, 126.9, 124.6, 117.8, 116.5, 111.5, 109.5, 69.1, 68.6, 31.4, 28.8, 25.7, 25.5, 22.4, 13.9, 13.8. MS (ESI): $m/z = 1559.4$. $\text{C}_{90}\text{H}_{105}\text{N}_{13}\text{O}_{12}$ ($M_w = 1560.88$): calcd. C, 69.25; H, 6.78; N, 11.67; found C, 69.43; H, 7.05; N, 11.32.

2.3. Fabrication and measurement of DSSCs

Photoelectrode preparation: The preparation of the photoelectrode was performed by adopting doctor-blade technique on

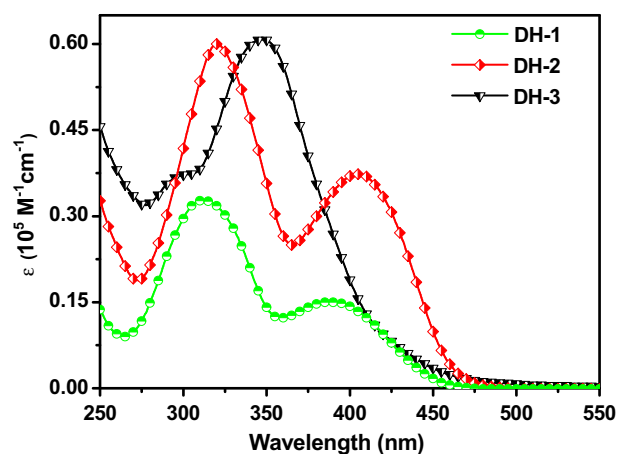
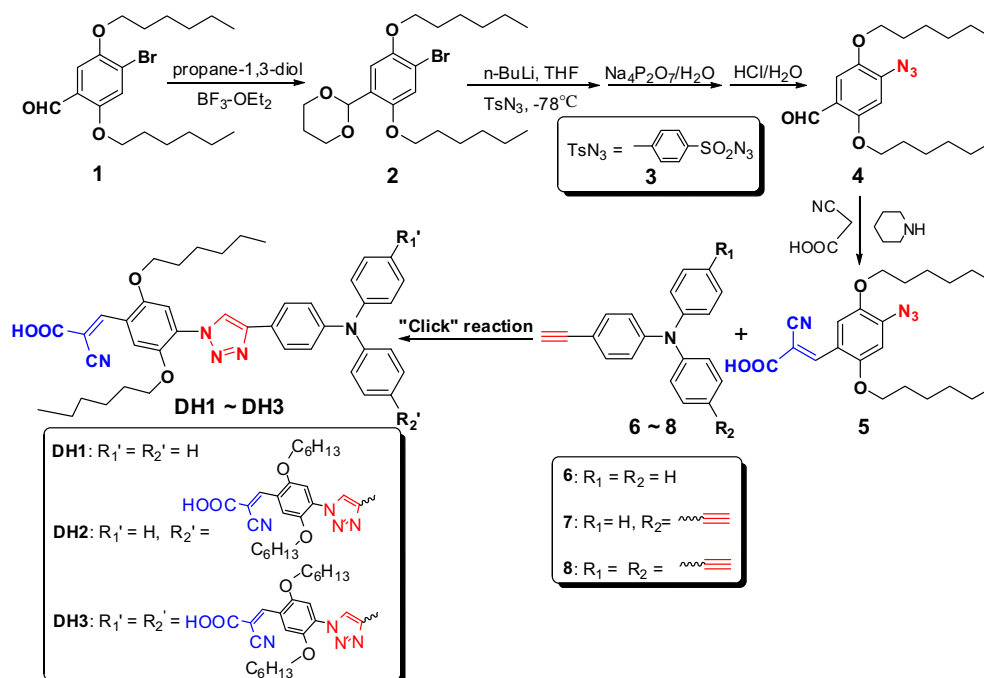


Fig. 2. UV-vis absorption spectra of **DH** dyes in solution of dioxane.

a conducting glass (FTO, 15–20 Ω/sq), which has been rinsed with distilled water and fully soaked in isopropanol for 3 h to increase its hydrophilicity before use.

The paste containing TiO_2 with a diameter of 13 nm (Ti-Nanoxide D, Solaronix) was spread on FTO glass. In order to obtain films with the same thickness, four pieces of FTO glasses with adhesive tape, which placed as spacers, were put in parallel when spreading the paste. The films were dried under mild condition and then annealed at 500 $^\circ\text{C}$ for 1 h. Finally the dye-sensitized electrodes were prepared by immersing the obtained films in mixed solution of dyes (ethanol/THF for **DH-1** and **DH-3**, ethanol/DMF for **DH-2** and N719 for ethanol, 3×10^{-4} mol/L of all) overnight.

DSSCs fabrication: The dye-sensitized electrode was assembled in a classic sandwich-type cell, that is, the platinum counter electrode was attached on the dye-sensitized photoanode. After the injection of the electrolyte solution, which consists of 0.5 M LiI, 0.05 M I_2 , and 0.1 M 4-tert-butylpyridine in 1:1 acetonitrile-propylene carbonate into the interspace between the photoanode



Scheme 1. The synthetic route for **DH-1**, **DH-2** and **DH-3** dyes.

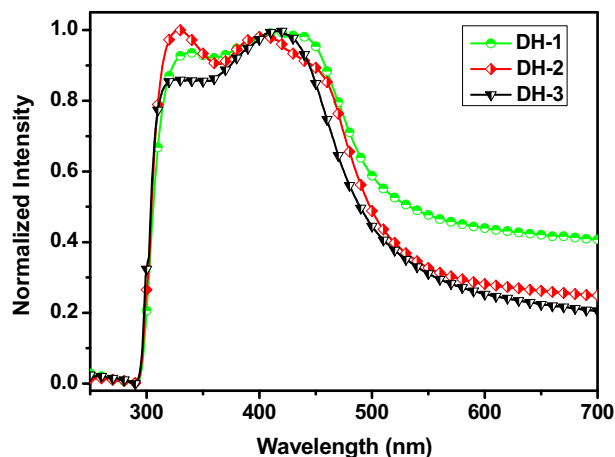


Fig. 3. UV–vis absorption spectra of **DH** dyes in solid adsorbed on TiO_2 film.

and the counter electrode, the photoelectrochemical property of the DSSC was measured.

DSSC evaluation: For the characteristic photocurrent–voltage (J – V) measurements, the DSSC was illuminated by light with energy of a 100 mW cm^{-2} (AM1.5) from a 300 W solar simulator (Newport, 91160). A computer-controlled Keithley 2400 source meter was employed to collect the J – V curves.

3. Results and discussion

The synthetic route for **DH-1**, **DH-2** and **DH-3** is depicted in Scheme 1. The azide intermediate **4** was obtained by nucleophilic substitution of 4-bromo-2,5-bis(hexyloxy)benzaldehyde with 4-methylbenzenesulfonyl azide in the presence of $n\text{-BuLi}$, in which the aldehyde group was initially protected by transforming it into acetal with 1,3-propylene glycol and then deprotected in dilute HCl. Later, cyanoacetic acid was linked with **4** through a Knoevenagel condensation to afford the intermediate **5**. The terminal alkynes (**6**, **7** and **8**) were synthesized by Sonogashira coupling reaction of 2-methylbut-3-yn-2-ol with the corresponding brominated triphenylamine derivatives and then by an acetone-elimination procedure, respectively. Finally, the target dyes (**DH-1**, **DH-2** and **DH-3**) were obtained in high yield via a ‘Click’ reaction of azide intermediate **5** with the terminal alkynes (**6**, **7** and **8**). In addition, the long-chain alkoxy group was present in the target molecules to improve the solubility. All the intermediates and **DH** dyes were characterized by standard spectroscopic methods and elemental analysis.

The UV–vis absorption spectra of the **DH** dyes in dilute dioxane solution ($1 \times 10^{-5} \text{ M}$) and in solid adsorbed on thin TiO_2 film are presented in Figs. 2 and 3, respectively. The corresponding data are summarized in Table 1.

As can be seen in Fig. 2, **DH-1** and **DH-2** exhibit obvious maximum absorption bands at two distinct regions. One is at about 310 nm corresponding to the π – π^* electron transition of the

Table 1
Photophysical properties of **DH** dyes.

DH dye	$\lambda_{\text{max}}^{\text{a}}$ (nm)	$\lambda_{\text{max}}^{\text{b}}$ (nm)	ϵ^{c} ($10^4 \text{ M}^{-1} \text{ cm}^{-1}$)
DH-1	312, 388	330, 420	3.28, 1.51
DH-2	320, 405	329, 405	6.00, 3.73
DH-3	348 (302) ^d	419	6.08

^a Absorption maximum in solution.

^b Absorption maximum adsorbed on TiO_2 thin film.

^c The molar extinction coefficient at λ_{max} in solution.

^d A shoulder peak.

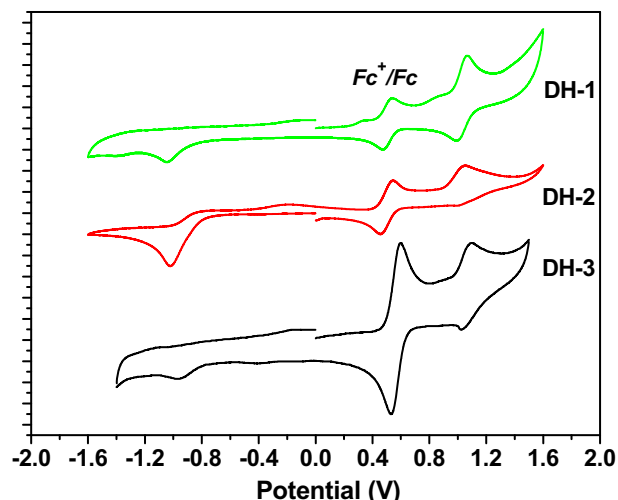


Fig. 4. Cyclic voltammograms of **DH** dyes with the Fc^+/Fc (Fc = ferrocene) couple as the internal standard.

localized conjugation skeleton, and the other is around 400 nm that can be assigned to an intramolecular charge transfer (ICT) between the central triphenylamine (electron-donor) and the cyanoacetic acid (electron-acceptor) anchoring moieties. As for **DH-3**, the absorption band of ICT occurs at around 350 nm and the π – π^* electron transition of the localized conjugation skeleton is only exhibited as a shoulder peak at about 300 nm. By comparison, it is found that the absorption maximum of ICT for **DH-1** and **DH-2** is clearly more red-shifted than that of **DH-3** since the strong molecular polarity of **DH-1** and **DH-2** favors the ICT electron delocalization. After being adsorbed on the surface of TiO_2 film, the UV–vis absorption of all **DH** dyes (shown in Fig. 3) shows a dramatic red-shift as compared to those in solution (especially the **DH-3** dye) and the absorption intensity in the range of 300–500 nm are significantly enhanced. This may be due to the increased delocalization of the π^* orbital of the conjugated framework caused by the interaction between the carboxylate group and the Ti^{4+} ions that directly decreases the energy of the π^* level. In addition, the introduction of long-chain alkoxy groups endow the **DH** dyes with a high extinction coefficient as shown in Table 1, suggesting that their light-harvesting should operate efficiently.

The redox behavior of **DH** dyes was studied by cyclic voltammetry (in Fig. 4) for the purpose to investigate the ability of electron transfer from the excited dye molecules to the conductive band of

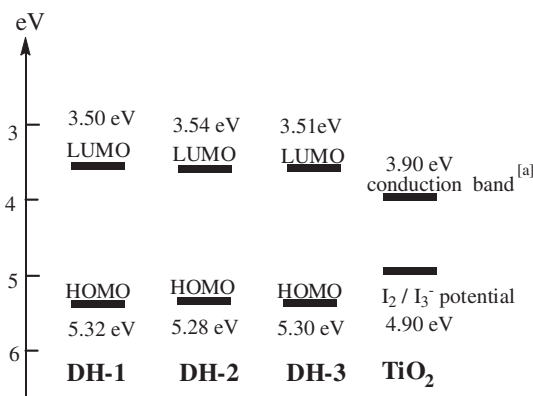


Fig. 5. Energy level diagrams of **DH** dyes from electrochemical data. ^[a] Refs. [22,23].

Table 2
Electrochemical properties of **DH** dyes.

DH dye	$E_{\text{red}}^{\text{a}}$ (V)	E_{ox}^{b} (V)	LUMO ^c (eV)	HOMO ^d (eV)	E_{gap} (eV)
DH-1	−0.86	0.96	−3.50	−5.32	1.82
DH-2	−0.83	0.91	−3.54	−5.28	1.74
DH-3	−0.81	0.98	−3.51	−5.30	1.99

^a Estimated from the onset reduction potential.

^b Estimated from the onset oxidation potential.

^c Calculated with the formula $E_{\text{LUMO}} = -[E_{\text{red}} + [4.8 - E_{(\text{Fc}/\text{Fc}^+)}]]\text{eV}$.

^d Calculated with the formula $E_{\text{HOMO}} = -[E_{\text{ox}} + [4.8 - E_{(\text{Fc}/\text{Fc}^+)}]]\text{eV}$.

TiO₂. The cyclic voltammograms of **DH** dyes were measured in a solution of 0.1 M *n*-Bu₄NPF₆ in DMF. A three-electrode cell containing a Pt-coil working electrode, a Pt wire counter electrode and a Ag/AgCl reference electrode was employed. The ferrocene/ferrocenium (Fc/Fc⁺) redox couple was used as an internal reference.

As can be seen in Fig. 4, all the **DH** dyes show the irreversible wave on the reduction side. The onset reduction potential around −0.80–0.86 V gives the LUMO energies of **DH** dyes around −3.50 eV, summarized in Table 2 which are higher than the TiO₂ conduction band (−3.9 eV) [22,23] as shown in Fig. 5. This indicates that the electron injection process is energetically favorable compared with the conduction band edge energy level of the TiO₂ electrode (−0.5 V vs NHE) [24]. The onset oxidation potential around 0.9 eV can be attributed to the oxidation of the TPA group. The HOMO energies around 5.30 eV (Table 2) are lower than the I/I⁺ potential, suggesting that there is enough driving force for the regeneration of the dye.

The frontier molecular orbitals (HOMO and LUMO) of the **DH** dyes at the B3LYP/6-31G level are shown in Fig. 6, and the surfaces are generated with an isovalue at 0.02. As can be seen, the electron density is uniformly distributed along the triphenylamine unit at the HOMO state; whereas at the LUMO level, excited electrons are shifted to the π -electron system of the anchor group (phenyl-substituted cyanoacrylic acid unit), which is due to the ICT along the π -conjugated skeleton. Therefore, it can be expected that the excited electron will be effectively injected into the conduction band of TiO₂ through the carboxyl anchor group as well as the adjacent electron-withdrawing cyano group. In addition, the results of calculation indicate that the introduction of the 1,2,3-triazole group favors spatial separation of HOMO and LUMO energy levels of the **DH** dyes. Generally, the good spatial separation and the twisted non-planar geometric structure of triphenylamine

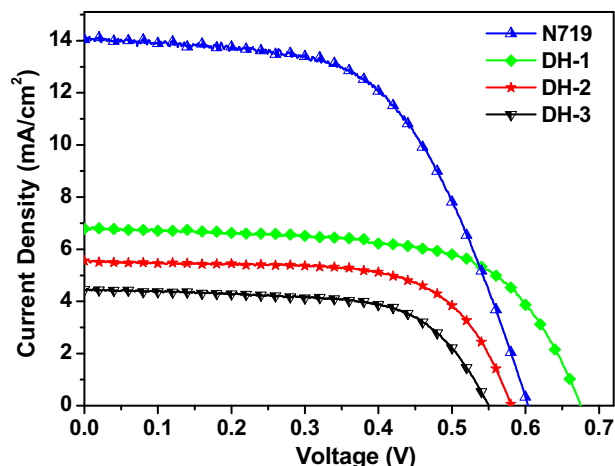


Fig. 7. Photocurrent density–photovoltage curves of **DH** dye-based cells.

unit can effectively suppress the charge recombination, and enhance the open-circuit voltage.

The photovoltaic properties of the solar cells based on **DH** dyes were measured under standard AM 1.5G irradiation. As shown in Fig. 7 and Table 3, all of the **DH** dyes have a comparable fill factor (*ff*) value, which is higher than that of the N719-based cell. However, the V_{oc} values of **DH** dyes is different and in the order of **DH-1** > **DH-2** > **DH-3** that decreases with increasing branches. The downtrend of V_{oc} is mostly associated with the positive shift of the conduction band (CB) edge of the TiO₂ photoanode [25] and inadequate control of charge recombination at the TiO₂/dye/electrolyte interface [26], which could be both caused by increasing anchor groups for series **DH** dyes. Similar phenomenon has been observed in the other triphenylamine-based organic dyes containing a thiophen bridge reported by Zhan et al. [27]. Since more protons are provided and transferred to the TiO₂ surface upon adsorption with the increment of anchoring groups in the **DH** dyes, they can charge the CB edge of the TiO₂ photoanode more positively and lead to a lower V_{oc} [27].

It has been reported that charge recombination can be decelerated by introducing the non-planar charge-separated structure [28,29] and the alkoxy chains can act as a suppression function of the charge recombination [30]. In addition, the introduction of

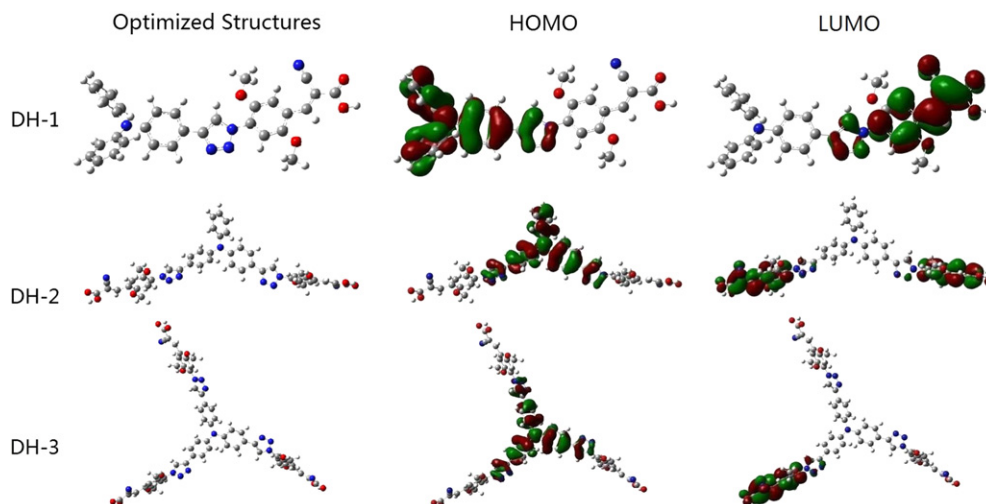


Fig. 6. The frontier HOMO and LUMO orbitals of **DH** dyes.

Table 3
Photovoltaic performances of DSSCs based on **DH** dyes and N719.

DH dye	V_{oc} (V)	J_{sc} (mA/cm ²)	ff	η (%)
DH-1	0.69	6.85	0.63	3.00
DH-2	0.59	5.56	0.65	2.13
DH-3	0.56	4.45	0.63	1.58
N719	0.61	14.04	0.57	4.86

electron-withdrawing 1,2,3-triazole group does favor the spatial charge separation in **DH** dyes. Thus, all DSSCs based on **DH** dyes show a relatively high V_{oc} value. Especially, the V_{oc} value of **DH-1**-based cell is even higher than that of the N719-based cell. However, the J_{sc} values of the **DH** dye cells are far from the N719-based cell device. The narrow absorption band of **DH** dyes is the crux of the problem. In addition, the electron-withdrawing 1,2,3-triazole structure, which seems to favor enhancing V_{oc} value, possibly hinders the electron injection into the CB of TiO₂ that is adverse to the generation of photocurrent. Indeed, from the point of view of practical application, **DH** dyes are not panchromatic, since only a narrow part of the solar spectrum is absorbed. However, this situation can be improved through modifying the structure such as to extend π -backbone in this similar family of dyes. The structural modification and optimal measurement of the photovoltaic properties for the series **DH** dyes are still in progress.

4. Conclusions

Three new metal-free organic dyes (**DH-1**, **DH-2** and **DH-3**) composed with different branched numbers of anchoring groups have been synthesized through a convenient 'Click' reaction. The introduction of the 1,2,3-triazole unit is favorable for the charge separation of the **DH** dyes, which can effectively suppress the charge recombination and increase the V_{oc} and fill factor of **DH**-based DSSCs. However, the introduction of more branched structure in the **DH** dyes makes the molecular polarity decrease that leads to the narrow and blue-shifted absorption and is unfavorable for the DSSCs performance. This work provides beneficial information for developing similar families of new organic dyes for DSSCs.

Acknowledgments

We are grateful to the National Natural Science Foundation of China (Nos. 20972122 and 20774071) and the Specialized Research Fund for the Doctoral Program of Higher Education of China (No. 20100141110010) for financial support.

References

- Regan BO, Grätzel M. A low-cost, high-efficiency solar cell based on dye-sensitized colloidal TiO₂ films. *Nature* 1991;353:737–40.
- Moreira Gonçalves L, de Zea Bermudez V, Aguilar Ribeiro H, Magalhães Mendes A. Dye-sensitized solar cells: a safe bet for the future. *Energy Environ Sci* 2008;1:655.
- Nazeeruddin MK, Klein C, Liska P, Grätzel M. Synthesis of novel ruthenium sensitizers and their application in dye-sensitized solar cells. *Coord Chem Rev* 2005;249:1460–7.
- Wang XF, Koyama Y, Kitao O, Wada Y, Sasaki S, Tamiaki H, et al. Significant enhancement in the power-conversion efficiency of chlorophyll co-sensitized solar cells by mimicking the principles of natural photosynthetic light-harvesting complexes. *Biosens Bioelectron* 2010;25:1970–6.
- Robertson N. Optimizing dyes for dye-sensitized solar cells. *Angew Chem Int Ed* 2006;45:2338–45.
- Mishra A, Fischer MKR, Bäuerle P. Metal-free organic dyes for dye-sensitized solar cells: from structure:property relationships to design rules. *Angew Chem Int Ed* 2009;48:2474–99.
- Chen CY, Wang MK, Li JY, Pootrakulchote N, Alibabaei L, Ngoc-le CH, et al. Highly efficient light-harvesting ruthenium sensitizer for thin-film dye-sensitized solar cells. *ACS Nano* 2009;3:3103–9.
- Li RZ, Liu JY, Cai N, Zhang M, Wang P. Synchronously reduced surface states, charge recombination, and light absorption length for high-performance organic dye-sensitized solar cells. *J Phys Chem B* 2010;114:4461–4.
- Ooyama Y, Harima Y. Molecular designs and syntheses of organic dyes for dye-sensitized solar cells. *Eur J Org Chem* 2009;18:2891.
- Qin H, Wenger S, Xu M, Gao F, Jing X, Wang P, et al. An organic sensitizer with a fused dithienothiophene unit for efficient and stable dye-sensitized solar cells. *J Am Chem Soc* 2008;130:9202.
- Yum JH, Hagberg DP, Moon SJ, Karlsson KM, Marinado T, Sun LC, et al. A light-resistant organic sensitizer for solar-cell applications. *Angew Chem Int Ed* 2009;48:1576–80.
- Zhang GL, Bala H, Cheng YM, Shi D, Lv XJ, Yu QJ, et al. High efficiency and stable dye-sensitized solar cells with an organic chromophore featuring a binary π -conjugated spacer. *Chem Commun* 2009;16:2198–200.
- Im H, Kim S, Park C, Jang SH, Kim CJ, Kim K, et al. High performance organic photosensitizers for dye-sensitized solar cells. *Chem Commun* 2010;46:1335–7.
- Zeng WD, Cao YM, Bai Y, Wang YH, Shi YS, Zhang M, et al. Efficient dye-sensitized solar cells with an organic photosensitizer featuring orderly conjugated ethylenedioxythiophene and dithienosilole blocks. *Chem Mater* 2010;22:1915–25.
- Rostovtsev VV, Green LG, Fokin VV, Sharpless KB. A stepwise Huisgen cycloaddition process: copper(I)-catalyzed regioselective "Ligation" of azides and terminal alkynes. *Angew Chem Int Ed* 2002;41:2596.
- Michinobu T. Click-type reaction of aromatic polyamines for improvement of thermal and optoelectronic properties. *J Am Chem Soc* 2008;130:14074–5.
- Fazio MA, Lee OP, Schuster DL. First triazole-linked porphyrin-fullerene dyads. *Org Lett* 2008;10:4979–82.
- Li ZA, Yu G, Wu WB, Liu YQ, Ye C, Qin JG, et al. Nonlinear optical dendrimers from click chemistry: convenient synthesis, new function of the formed triazole rings, and enhanced NLO. *Effects Macromolecules* 2009;42:3864–8.
- Wen SP, Pei JN, Zhou YH, Li PF, Xue LL, Li YW, et al. Synthesis of 4,7-diphenyl-2,1,3-benzothiadiazole-based copolymers and their photovoltaic applications. *Macromolecules* 2009;42:4977–84.
- Djukic JP, Michon C, Heiser D, Kyritsakas-Gruber N, de Cian A, Dotz KH, et al. The reaction of diazocyclopentadienyl compounds with cyclomanganated arenes as a route to ligand-appended cymantrenes. *Eur J Inorg Chem* 2004;10:2107.
- Meng FS, Li J, Tian H, Su JH, Li W. Method for synthesis of red light-emitting naphthalimide compound. CN Patent 2005; CN1616429 (A).
- Lenzmann F, Krueger J, Burnside S, Brooks K, Grätzel M, Gal D, et al. Surface photovoltage spectroscopy of dye-sensitized solar cells with TiO₂, Nb₂O₅, and SrTiO₃ nanocrystalline photoanodes: indication for electron injection from higher excited dye states. *J Phys Chem B* 2001;105:6347–52.
- Kumaresan D, Thummel RP, Bura T, Ulrich G, Ziesler R. Color tuning in new metal-free organic sensitizers (bodipys) for dye-sensitized solar cells. *Chem Eur J* 2009;15:6335–9.
- Wang ZS, Cui Y, Dan-Oh Y, Kasada C, Shinpo A, Hara K. Molecular design of coumarin dyes for stable and efficient organic dye-sensitized solar cells. *J Phys Chem C* 2008;112:17011–7.
- Nazeeruddin MK, Zakeeruddin SM, Humphry-Baker R, Jirousek M, Liska P, Vlachopoulos N, et al. Acid-base equilibria of (2,2'-Bipyridyl-4,4'-dicarboxylic acid)ruthenium(II) complexes and the effect of protonation on charge-transfer sensitization of nanocrystalline titania. *Inorg Chem* 1999;38:6298–305.
- Haque SA, Palomares E, Cho BM, Green ANM, Hirata N, Klug DR, et al. Charge separation versus recombination in dye-sensitized nanocrystalline solar cells: the minimization of kinetic redundancy. *J Am Chem Soc* 2005;127:3456–62.
- Shang H, Luo Y, Guo X, Huang X, Zhan X, Jiang K, et al. The effect of anchoring group number on the performance of dye-sensitized solar cells. *Dyes Pigm* 2010;87:249–56.
- Ozeki H, Nomoto A, Ogawa K, Kobuke Y, Murakami M, Hosoda K, et al. Role of the special pair in the charge-separating event in photosynthesis. *Chem Eur J* 2004;10:6393–401.
- Velusamy M, Thomas KRJ, Lin JT, Hsu YC, Ho KC. Organic dyes incorporating low-band-gap chromophores for dye-sensitized solar cells. *Org Lett* 2005;7:1899–902.
- Xu MF, Li RZ, Pootrakulchote N, Shi D, Guo J, Yi ZH, et al. Tuning the energy level of organic sensitizers for high-performance dye-sensitized solar cells. *J Phys Chem C* 2008;112:19770–6.